INTERNATIONAL JOURNAL OF PRECISION ENGINEERING AND MANUFACTURING Vol. 16, No. 8, pp. 1789-1800 JULY 2015 / 1789
DOI: 10.1007/s12541-015-0234-7 ISSN 2234-7593 (Print) / ISSN 2005-4602 (Online)

A Modified Method of the Unified Jacobian-Torsor Model for Tolerance Analysis and Allocation

Hua Chen[1,#], Sun Jin[1,2], Zhimin Li[1], and Xinmin Lai[1,2]

1 Shanghai Key Laboratory of Digital Manufacture for Thin-walled Structures, Shanghai Jiao Tong University, 800 Dongchuan RD, Minhang District, Shanghai, 200240, China
2 State Key Laboratory of Mechanical System and Vibration, Shanghai Jiao Tong University, 800 Dongchuan RD, Minhang District, Shanghai, 200240, China
Corresponding Author / E-mail: chenhua@sjtu.edu.cn, TEL: +86-021-34206306, FAX: +86-021-34206306

KEYWORDS: Component, Variation, Constraint, Torsor model, Tolerance analysis, Allocation

The unified Jacobian-Torsor model uses the torsor model for tolerance representation and the Jacobian matrix for tolerance propagation. The torsor model is composed of six components, i.e., three translational vectors and three rotational vectors. However, previous studies about this model have only considered the constraint of individual component. In fact, this constraint is the scope of a single component. It is called variation. Relations between these components are constraints which reflect the interaction between them in a tolerance zone. Integrating all limited values of components of torsors into the unified Jacobian-Torsor model may lead to an inaccurate result. Meanwhile, the variations and constraints of torsor for a feature specified by more than one tolerance have been not illustrated clearly. In this paper, a modified method of the unified Jacobian-Torsor model considering constraints between components of torsor is presented. The variations and constraints of torsors for cylindrical and planar features are proposed. These constraints are calculated by means of a modified Monte Carlo method based on the previous work. Moreover, tolerance allocation of this modified method in a statistical way is also introduced. Two case studies have been performed to demonstrate the modified method.

Manuscript received: September 26, 2014 / Revised: November 27, 2014 / Accepted: April 22, 2015

1. Introduction

With the ever-tightening and complex requirements of tolerance analysis in industrial fields, tolerance analysis methods have developed from traditional one/two dimensional (1/2D) to three dimensional (3D). Distinguishing and quantifying the roles of dimensional and geometric tolerances specified on a feature and their interactions which can not be handled by 1/2D methods, are the major advantages of 3D tolerance analysis methods. These merits are very important to tolerance specification and allocation for complex mechanisms. Taking the engine shown in Fig. 1 as an example, the dimensional and geometric tolerances of crank-link mechanism will propagate to the piston through joints between parts. The translational (Dt) and rotational ($D\alpha$) variations of the piston have great influences on compression ratio of engines. Taking the dimensional and geometric tolerances and their interactions into account will produce a more accurate result than considering dimensional tolerances only. Meanwhile, these tolerances also affect other performances, such as frictional work and sealing. 3D tolerance analysis can offer a significant clue for tolerance specification and allocation of engine design.

3D tolerance analysis methods are innovative technologies which represent and transfer tolerance in 3D Euclidean space.[1-3] Geometric tolerances and dimensional tolerances, as well as the interaction between them can be taken into consideration by these methods. Over the last decades, many 3D models based on literature have been proposed.[4,5] Preliminary explorations include the spatial dimensional chain,[6] the network of zones and datums,[7] and the kinematic formulation.[8] After that, the Jacobian matrix,[9] the T-Map model,[10] the direct linearization method (DLM),[11] the torsor model,[12,13] the matrix model,[14] and the unified Jacobian-Torsor model[15] have been presented successively. It should be pointed out that the concept of 3D tolerance analysis here mainly focuses on tolerance representation and propagation in assemblies. Tolerance representation and propagation in manufacturing are totally different from assemblies. Therefore, some 3D tolerance analysis models used in manufacturing, such as the state space method,[16] the analysis line method,[17] and the variational method,[18] are not discussed here.

Four major models mentioned above, i.e., the T-Map model, the matrix model, the DLM and the unified Jacobian-Torsor model, are reported largely and studied deeply in literature. Brief comments about each method are listed as follows.

The T-Map® (Patent No. US6963824) model, developed by

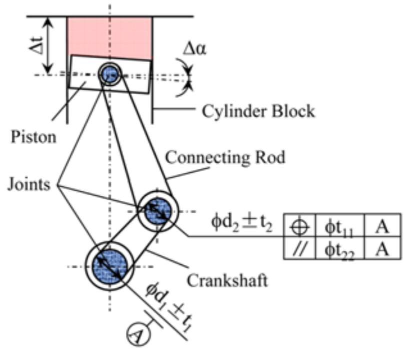

Fig. 1 A crank-link mechanism of engine

Davidson et al.,[10,19] is a hypothetical Euclidean volume of points, shape, size, and internal subsets of which represent all possible variations in size, position, form, and orientation of a target feature. Besides round and polygonal surfaces, T-Maps have been developed for other features, such as axes,[20-22] angled faces,[23] point-line clusters,[24] planar and radial clearances in a statistical way.[25-27] The T-Map model is fully consistent with the ASME standard and suitable for tolerance allocation. However, the Minkowski operation of T-Map for tolerance propagation and the visualization of higher dimensional maps are not straightforward. In other words, T-Map has not yet been fully developed.

The matrix model introduced by Desrochers and Rivière[14] uses a displacement matrix to describe small displacements of a feature within its tolerance zone and clearance between two features. A 4×4 homogeneous matrix including a 3×3 rotational matrix and a 3×1 translational matrix is chosen to represent the relative displacements of a feature within its tolerance zone. Tolerance propagation of the matrix model depends on homogeneous matrixes of assemblies. A matrix model is completed by a set of inequalities defining the bounds of every component of matrix. These inequalities depend on features and tolerances. A statistical method of the matrix model has also been given.[28] Although it is very suitable for tolerance analysis of planar and cylindrical surfaces, a large number of constraint inequalities, especially non-linear inequalities, make the computation process difficult and time-consuming.

The DLM proposed by Chase et al.[11,29] is based on the first order Taylor's series expansion of vector-loop-based assembly models which use vectors to represent either component dimensions or assembly dimensions. Geometric tolerances are considered by placing at the contact point between mating surfaces with zero length vectors.[30] Sensitivity matrixes obtained from vector-loops are used in tolerance calculation. Moreover, the second order tolerance analysis (SOTA) method has been developed to enhance the accuracy of DLM.[31] Although all types of tolerances can be modeled, and the deterministic and statistical results can be calculated efficiently, how to define the joint types and the effects of geometric variations are dependent of user's choices. It is also worth mentioning that the interaction between geometric tolerance and dimensional tolerance is indistinct.

The unified Jacobian-Torsor model introduced by Desrochers et al.[15] is an innovative tolerance analysis method which uses the torsor model for tolerance representation and the Jacobian matrix for tolerance propagation. Both deterministic and statistical analysis methods about this model are concise and efficient.[32,33] Moreover, tolerance allocation of this model in a deterministic way has been studied preliminarily.[34] For complex assemblies which contain a large number of joints and geometric tolerances, such as engines, the unified Jacobian-Torsor model is more suitable theoretically.

The torsor model is composed of six components, i.e., three translational vectors and three rotational vectors. However, the presented deterministic and statistical methods of this model have only considered the constraint of individual component of torsor. In fact, this constraint is the scope of a single component. It is called variation. Relations between these components are constraints which reflect the interaction between them in a tolerance zone. According to the ASME standard,[35] there are actually interactions between translational vectors and rotational vectors in a tolerance zone. Integrating limited values of both rotational and translational vectors into account would be inaccurate. Meanwhile, how to define the variations and constraints of torsor for a feature specified by more than one tolerance has not been illustrated clearly. The interaction of combinational tolerances is complex because of involving tolerancing standards.

In this paper, a modified method of the unified Jacobian-Torsor model considering constraints between components of torsor is presented. The variations and constraints of torsors for cylindrical and planar features specified by combinational tolerances are proposed. These constraints are calculated by means of the modified Monte Carlo method based on the previous work. Meanwhile, tolerance allocation of this modified method in a statistical way is also introduced. The modified method has been illustrated by a crank-link mechanism of engine and a two-block assembly. The accuracy of the unified Jacobian-Torsor model is improved by more than 7%, while the computational efficiency is without any loss.

The rest of the paper is organized as follows. Section 2 provides a review of the unified Jacobian-Torsor model and its statistical method. Section 3 presents the modified method of the unified Jacobian-Torsor model considering the constraints between components of torsor. The mathematic models of variations and constraints of torsors for cylindrical and planar features specified with more than one tolerance, as well as their joints are proposed. The solution and tolerance allocation of this modified method are also introduced. Section 4 illustrates this modified method by two examples. Section 5 presents comparison and discussion. Section 6 is conclusions.

2. Unified Jacobian-Torsor Model

The torsor, also known as the small displacement torsor (SDT) in the field of tolerance analysis, is used to represent position and orientation of an ideal surface or its feature (axis, center, plane) in relation to another ideal surface in a kinematic way.[36] As shown in Fig. 2, at a given point on nominal surface S_0, the torsor of variational surface S_1 from S_0 can be expressed as:

$$T = \begin{bmatrix} \alpha & u \\ \beta & v \\ \gamma & w \end{bmatrix} \quad (1)$$

where α, β and γ are rotational vectors around the axes x, y and z in

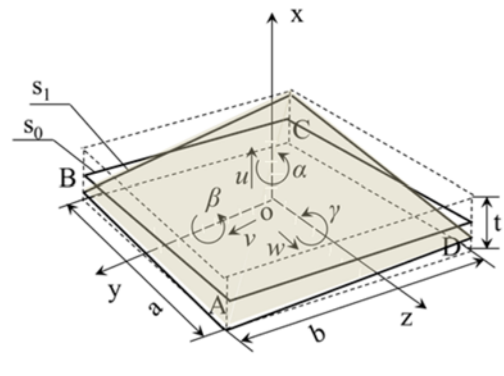

Fig. 2 Torsor model of a planar surface in its tolerance zone

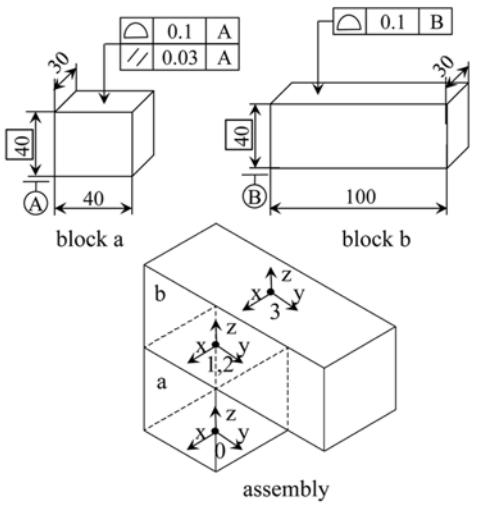

Fig. 3 A two-block assembly

local reference frame respectively; likewise, $\boldsymbol{u}$, $\boldsymbol{v}$, $\boldsymbol{w}$ are translational vectors along the axes x, y and z respectively.

Tolerances are only meaningful in direction other than those that leave a surface invariant with respect to itself,[37] which means that the number of effective components in a torsor model is equal to the non-invariant degree of a feature. Therefore, $\boldsymbol{v}$, $\boldsymbol{w}$ and α in Fig. 2 and Eq. (1) can be set as zero to simplify the computational process.

Tolerance representation with the torsor model is concise and intuitionistic, but it is difficult for tolerance transfer.[38,39] Therefore, the Jacobian matrix is introduced into tolerance analysis.

There are two types of functional pairs in assembly, i.e., internal pair and contact or kinematic pair. The former is composed of two functional elements (FEs) on the same part; the latter is consists of two FEs on different parts if there is a physical or potential contact between them. The Jacobian matrix for the ith FE can be expressed as:

$$[J]_{FEi} = \begin{bmatrix} [R_0^i]_{3\times3}\cdot[R_{Pti}]_{3\times3} & \cdots & [W_i^n]_{3\times3}\cdot([R_0^i]_{3\times3}\cdot[R_{Pti}]_{3\times3}) \\ \cdots & \cdots & \cdots \\ [0]_{3\times3} & \cdots & [R_0^i]_{3\times3}\cdot[R_{Pti}]_{3\times3} \end{bmatrix} \quad (2)$$

where R_0^i represents the local orientation of the ith reference frame with respect to the 0th reference frame that is the global reference system; R_{Pti} is a projection matrix designating the unit vectors along local axes respectively for tolerance zone tilted according to the direction of tolerance analysis; W_i^n is a skew-symmetric matrix allowing the representation of the vector among the ith and nth (end point) reference frames, defined as Eq. (3); $W_i^n\cdot R_0^i$ reflects the leverage effect when the small rotations are being multiplied by these terms of the Jacobian matrix.

$$[W_i^n]_{3\times3} = \begin{bmatrix} 0 & dz_i^n & -dy_i^n \\ -dz_i^n & 0 & dx_i^n \\ dy_i^n & -dx_i^n & 0 \end{bmatrix} \quad (3)$$

where $dx_i^n = dx_n - dx_i$, $dy_i^n = dy_n - dy_i$, $dz_i^n = dz_n - dz_i$.

The torsor model is suitable for tolerance representation while the Jacobian matrix is good at tolerance propagation. The unified Jacobian-Torsor model combines the advantages of both. The final expression of a unified Jacobian-Torsor model can be written as follows:

$$\begin{bmatrix} (\underline{u},\overline{u}) \\ (\underline{v},\overline{v}) \\ (\underline{w},\overline{w}) \\ (\underline{\alpha},\overline{\alpha}) \\ (\underline{\beta},\overline{\beta}) \\ (\underline{\gamma},\overline{\gamma}) \end{bmatrix}_{FR} = [[J]_{FE1} \ \cdots \ [J]_{FEn}]\times\begin{bmatrix}\begin{bmatrix} (\underline{u},\overline{u}) \\ (\underline{v},\overline{v}) \\ (\underline{w},\overline{w}) \\ (\underline{\alpha},\overline{\alpha}) \\ (\underline{\beta},\overline{\beta}) \\ (\underline{\gamma},\overline{\gamma}) \end{bmatrix}_{FE1} & \cdots & \begin{bmatrix} (\underline{u},\overline{u}) \\ (\underline{v},\overline{v}) \\ (\underline{w},\overline{w}) \\ (\underline{\alpha},\overline{\alpha}) \\ (\underline{\beta},\overline{\beta}) \\ (\underline{\gamma},\overline{\gamma}) \end{bmatrix}_{FEn}\end{bmatrix}^T \quad (4)$$

where FR represents functional requirement; $(\underline{\alpha},\overline{\alpha})$ is tolerance interval where α must lie in; other components of torsors follow the same way as α. Interval arithmetic is incorporated into Eq. (4) to allow tolerance analysis to be performed on a "tolerance zone basis" rather than on a "point basis".

A statistical method of the unified Jacobian-Torsor model has been proposed by Ghie et al.[33] The intervals in Eq. (4) become constraints for the generation of random values for each component in every torsor. Monte Carlo simulation is used to take all of random values into computation. The statistical method is computational effectively.

As can be seen, the unified Jacobian-Torsor model, no matter in a deterministic or statistical way, is easily integrated in computer programs. Meanwhile, tolerance allocation of this model in a deterministic way has been studied preliminarily.[34]

The presented methods only consider the variations of individual components, but ignore the constraints between them. Still taking the plane shown in Fig. 2 as an example, the torsor model and their variations have been given in Ref. 40. Obviously, all components can not arrive at their limited values at the same time. γ and β must shrink to zero when $\boldsymbol{u}$ arrives at its limited value. Otherwise, S_1 will be out of the tolerance zone. This situation will bring down the accuracy and validity of analysis result. Let us illustrate this problem with a two-block assembly shown in Fig. 3. A global reference frame (0) and three local reference frames (1, 2, 3) are constructed in the middle of related surfaces. The FR is the accumulative tolerance of top surface of block b along the z axis, which is measured in the global reference frame.

There are two FEs in this assembly. They are internal FEs formed by the top and bottom surfaces of two blocks. Based on the work introduced above, we can obtain a unified Jacobian-Torsor model about the FR:

$$\begin{bmatrix}(\underline{u},\overline{u})\\(\underline{v},\overline{v})\\(\underline{w},\overline{w})\\(\underline{\alpha},\overline{\alpha})\\(\underline{\beta},\overline{\beta})\\(\underline{\gamma},\overline{\gamma})\end{bmatrix}_{FR}=\left[\begin{bmatrix}1&0&0&0&40&-30\\0&1&0&-40&0&0\\0&0&1&30&0&0\\0&0&0&1&0&0\\0&0&0&0&1&0\\0&0&0&0&0&1\end{bmatrix}_{FE1}\begin{bmatrix}1&0&0&0&0&0\\0&1&0&0&0&0\\0&0&1&0&0&0\\0&0&0&1&0&0\\0&0&0&0&1&0\\0&0&0&0&0&1\end{bmatrix}_{FE2}\right] \times\left[\begin{bmatrix}(0,0)\\(0,0)\\(-0.05,0.05)\\(-0.1/40,0.1/40)\\(-0.1/30,0.1/30)\\(0,0)\end{bmatrix}_{FE1}\begin{bmatrix}(0,0)\\(0,0)\\(-0.05,0.05)\\(-0.1/100,0.1/100)\\(-0.1/30,0.1/30)\\(0,0)\end{bmatrix}_{FE2}\right]^T \quad (5)$$

Computational results in a deterministic way show that $\boldsymbol{w}$ in FR, i.e., the accumulative tolerance of top surface of block b along the z axis is ±0.1750. However, the result of this assembly obtained from traditional 1D tolerance chain is ±0.1. The absolute residual gap between these two methods is 0.075. It is a product of the rotational component (0.1/40) of FE1 and the distance 30 of $\boldsymbol{J_{FE1}}$. This gap is due to the so called leverage effect.

Eq. (5) takes limit values of all translational and rotational components into calculation. It ignores the interaction between them. The accuracy and validity of analysis result are dubious. Meanwhile, the role of the parallelism tolerance (0.03) is not considered. Therefore, it is necessary to explore a new method which can consider constraints between components of torsors to improve the accuracy and validity of the unified Jacobian-Torsor model.

3. Modified Method of Unified Jacobian-Torsor Model

Considering constraints between components of torsor in the unified Jacobian-Torsor model, means that the components of each torsor in Eq. (4) are not independent any more. They are bounded by variations and constraints. To integrate constraints into the unified Jacobian-Torsor model, we proposed a modified method based on Eq. (4):

$$\begin{bmatrix}(\underline{u},\overline{u})\\(\underline{v},\overline{v})\\(\underline{w},\overline{w})\\(\underline{\alpha},\overline{\alpha})\\(\underline{\beta},\overline{\beta})\\(\underline{\gamma},\overline{\gamma})\end{bmatrix}_{FR}=[[J]_{FE1}\ \dots\ [J]_{FEn}]\times\begin{bmatrix}\left[\begin{bmatrix}u_1\\v_1\\w_1\\\alpha_1\\\beta_1\\\gamma_1\end{bmatrix} S.t_1\begin{cases}V_1(u_1,v_1,w_1,\alpha_1,\beta_1,\gamma_1)\\C_1(u_1,v_1,w_1,\alpha_1,\beta_1,\gamma_1)\end{cases}\right]_{FE1}\\ \dots \\ \left[\begin{bmatrix}u_n\\v_n\\w_n\\\alpha_n\\\beta_n\\\gamma_n\end{bmatrix} S.t_n\begin{cases}V_n(u_n,v_n,w_n,\alpha_n,\beta_n,\gamma_n)\\C_n(u_n,v_n,w_n,\alpha_n,\beta_n,\gamma_n)\end{cases}\right]_{FEn}\end{bmatrix} \quad (6)$$

where $S.t_i$ represents constraint conditions; V_i and C_i are variations and constraints of the ith torsor respectively.

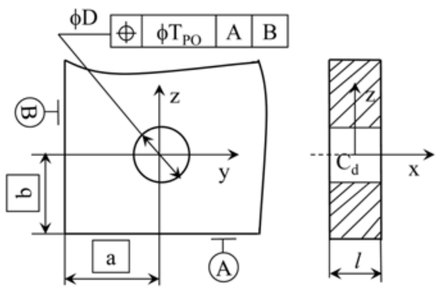

Fig. 4 Positional tolerance of a cylindrical feature

As can be seen, the modified method depends on two key factors. One is the variations and constraints of torsor decided by features and tolerances. Because of involving the tolerance principles, it is complicated when combinational tolerances are specified on a feature. Another is the solution of FR under the constraint conditions. They will be described in detail in the next subsections.

3.1 Variations and constraints

Tolerance specification for a target feature includes not only size and positional tolerance, but also orientation and form tolerances. Generally, form tolerances do not produce any effect in the unified Jacobian-Torsor model because the features are considered with nominal shape.[39] Two usual features are considered here.

3.1.1 Cylindrical feature

A cylindrical feature is composed of an integral feature (surface) and a derived feature (median line). Generally, the integral feature is specified by a dimensional tolerance while the derived feature is specified with positional and orientation tolerances. The dimensional tolerance restricts the size of the cylindrical surface, which affects its assembly joint. The positional tolerance and orientation tolerance restrict the position and orientation of the derived feature.

A cylinder has two invariant degrees, i.e., around and along its axis. Therefore, the cylindrical feature has four non-zero components of torsor. Let us consider a hole specified with a positional tolerance, as depicted in Fig. 4. The positional tolerance zone is a cylinder located at theoretical position relative to datum A and B, which is shown in Fig. 5. The vector equation about this tolerance zone can be expressed as:[41]

$$|C_d\times(P-C_P)|\le\frac{T_{PO}}{2} \quad (7)$$

where $\boldsymbol{C_d}$ and $\boldsymbol{C_p}$ are orientation and location vectors of the positional tolerance zone; T_{PO} is the value of the positional tolerance; $\boldsymbol{P}$ is a location vector of any point at the tolerance zone.

The local reference frame of the hole is constructed as Fig. 4. Then $C_d=[1\ 0\ 0]^T$ and $C_P=0$, the constraints about median line can be written as:

$$(v+\gamma x)^2+(w+\beta x)^2\le\left(\frac{T_{PO}}{2}\right)^2 \quad (8)$$

And the variations are $\{-T_{PO}/2l\le\beta\le T_{PO}/2l,\ -T_{PO}/2l\le\gamma\le T_{PO}/2l,\ -T_{PO}/2l\le v\le T_{PO}/2l,\ -T_{PO}/2l\le w\le T_{PO}/2l\}$.
where l is the length of the cylinder; $x\le l$.

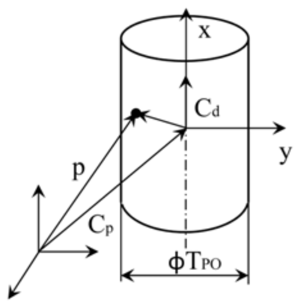

Fig. 5 Positional tolerance of an integral feature

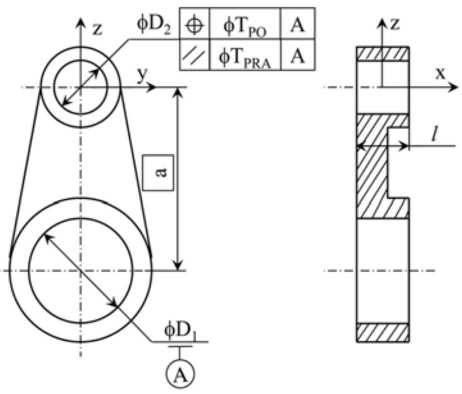

Fig. 6 Positional tolerance with parallelism tolerance for a cylinder

Eq. (8) and its variations describe the variations of β, γ, $\boldsymbol{v}$ and $\boldsymbol{w}$, as well as the constraints between them. As can be seen, β and γ must shrink to zero when $\boldsymbol{v}$ and $\boldsymbol{w}$ arrives at their limit values ($T_{PO}/2$).

Other positional tolerances of cylindrical features, such as concentricity, have similar constraints and variations equations with this positional tolerance.

Generally, more than one tolerance is needed for a feature in a precise mechanism. As shown in Fig. 6, a parallelism tolerance is specified to control the rotational range of axis of hole, besides the positional tolerance. According to the Rule #1 (Envelop Principle) of ASME standard, $T_{PRA} < T_{PO}$, and the rotational displacements of axis caused by T_{PRA} are restricted by T_{PO}. More specifically, rotations arrive at their minimal values (0) when translations arrive at their maximal values. Therefore, the constraints of the axis shown in Fig. 6 is same as Eq. (8), but the variations are rewritten as $\{-T_{PRA}/2l \le \beta \le T_{PRA}/2l, -T_{PRA}/2l \le \gamma \le T_{PRA}/2l, -T_{PO}/2l \le v \le T_{PO}/2l, -T_{PO}/2l \le w \le T_{PO}/2l\}$.

Other usual orientation tolerances combined with a positional tolerance on cylindrical surfaces can be deduced in the same way.

The contact pair or joint between cylindrical surfaces has relative movements if they form a clearance fit. Let us consider a clearance fit case formed by two coaxial cylinders (see Fig. 7), the amount of clearance can be expressed as Eq. (9). Here we deem that the effect of clearance is equal to a positional tolerance. The constraints of the joint shown in Fig. 7 can be expressed as Eq. (8) where T_{PO} is substituted by T_C.

$$T_C = (D+t_2)-(d-t_1) \tag{9}$$

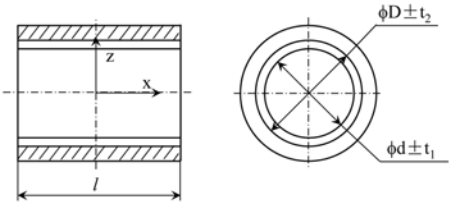

Fig. 7 Clearance formed by two cylindrical surfaces

It should be noted that the envelop principle for cylindrical features mainly focuses on the interaction between positional tolerance and orientation tolerance. The role of dimensional tolerance is the formation of joint described in Eq. (9). According to the envelop principle, the rotational displacements caused by geometric tolerances must arrive at their minimal value (0) when the translational displacements caused by dimensional or positional tolerances arrive at their maximal value. Therefore, it is reasonable to take dimensional tolerance and other two geometric tolerances into consideration separately.

3.1.2 Planar feature

A plane has three invariant degrees. Therefore, the variations and constraints of torsor about planar features are simple since the number of effective components of this torsor is only three. Furthermore, the joint of planar features is neglected because there is no relative movement in reality. Roy et al.[42] gave the detailed mathematic deduction of the variations and constraints of planar feature specified by size and orientation tolerances. Two cases are presented to illustrate the constraint relations briefly.

For a size tolerance, there are two types of tolerance specification. Type I is single direction toleranced in relation to a datum. Type II is both directions toleranced. Here we focus on type I because it is simple and fit for geometric tolerances. As shown in Fig. 8, the constraints about variant plane are:

$$-(T_{SU}+T_{SL}) \le (\beta z+\gamma y) \le (T_{SU}+T_{SL}) \tag{10}$$

$$-T_{SL} \le (u+\beta z+\gamma y) \le T_{SU} \tag{11}$$

And the variations are $\{-(T_{SU}+T_{SL})/a \le \beta \le (T_{SU}+T_{SL})/a, -(T_{SU}+T_{SL})/b \le \gamma \le (T_{SU}+T_{SL})/b, -T_{SL} \le u \le T_{SU}\}$.
where T_{SU} and T_{SL} are upper bound and lower bound values of the size tolerance.

If the target feature is specified with an orientation tolerance besides a size tolerance, for example, a parallelism tolerance T_{PRA} is specified besides T, according to the ASME standard, the constraints are rewritten as:

$$-\frac{T_{PRA}}{2} \le (\beta z+\gamma y) \le \frac{T_{PRA}}{2} \tag{12}$$

$$-T_{SL} \le (u+\beta z+\gamma y) \le T_{SU} \tag{13}$$

And the variations become $\{-T_{PRA}/a \le \beta \le T_{PRA}/a, -T_{PRA}/b \le \gamma \le T_{PRA}/b, -T_{SL} \le u \le T_{SU}\}$.

Other orientation tolerances, such as angularity and perpendicularity,

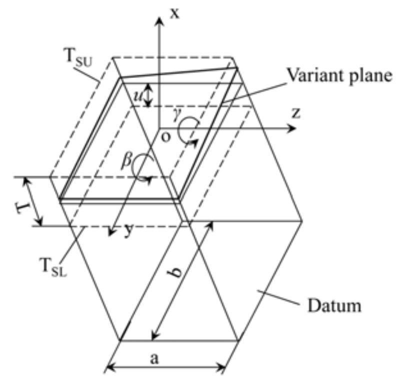

Fig. 8 Variational model of a planar surface

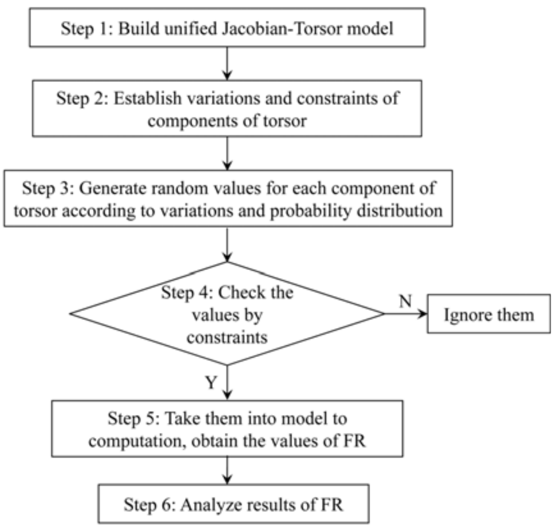

Fig. 9 Scheme used for modified unified Jacobian-Torsor model

have similar equations with the parallelism tolerance.

As can be seen, orientation tolerances mainly restrict the rotational displacements, and positional or size tolerances limit the translational displacements. There are strong interactions between them, which means the values of six components of torsor depend on each other.

3.2 Solution

In order to solve Eq. (6), we proposed a modified computational scheme based on the work of Ghie et al.,[33] as shown in Fig. 9. Monte Carlo method is still used here. But the values of components of torsors are verified before each simulation to ensure all of them satisfy the constraint conditions.

More specifically, the modified algorithm consists of the following steps.

Step 1: Build the expression of the unified Jacobian-Torsor model. The work includes FEs and FR identification, reference frames foundation and the Jacobian matrix establishment.

Step 2: Establish variations and constraints of torsors. According to functional elements and their tolerances, or joint types, the variations and constraints of torsors can be established.

Step 3: Generate random values for each component of every torsor. The variations in step 2 are used for the generation of random values for each component in every torsor. A desired statistical distribution is provided for each component with a specified percentage of rejection. For normal distribution, the mean and standard deviation of each component can be obtained by Eqs. (14)-(15) where the reject rate is assigned by designers.

$$\mu_T = \frac{V_{SU} - V_{SL}}{2} \tag{14}$$

$$\sigma_T = \frac{V_{SU} - \mu_T}{Z} \quad \text{or} \quad \sigma_T = \frac{\mu_T - V_{SL}}{Z} \tag{15}$$

where V_{SU} and V_{SL} are upper and lower limited variations of component. Z is the standardised normal value.

It should be noted that equations above are based on the assumption that the component distributions are normal. If the distributions are other than normal, appropriate levels and weights can be chosen to make a modification for them.[43]

Step 4: Check the random values with constraints equations obtained in step 2. This step selects the qualified values of components according to constraint relations to make sure that all computational variables are valid.

Step 5: Take the random values selected in step 4 into model to computer the results of FR. The number of iterations depends on the requirement of design. Generally, the larger the number of iterations is assigned, the more accurate the results, and the more time-consuming the computation.

Step 6: Analyze results of FR. Important parameters such as the mean and standard deviation of FR are obtained. The test of significance of distribution for results is carried out if necessary.

These six steps ensure that every component of torsor participating in computation is valid and compatible with the ASME standard. In essence, the modified method considers constraints between components of torsor in a statistical way, which is more beneficial to tolerance allocation and manufacturing. Variations and constraints γ of and $\boldsymbol{u}$ shown in Fig. 2 can be illustrated in Fig. 10. Fig. 10(a) shows that these two vectors are independent of each other. The constraints between them have been built (solid line) in Fig. 10(b). If a parallelism tolerance t_1 is specified besides t, will shrink (solid line), as shown in Fig. 10(c). For an actual tolerance zone, we consider that each component of torsor spans a $Z \cdot \sigma$ (Z is explained in Eq. (15)) range of normal distribution. Therefore, constraints are effective in a more concentrated area (black ellipse), as shown in Fig. 10(d).

Tolerance allocation or optimization can be carried out after tolerance analysis. It is based on a reverse deduction of the analysis model. There are two important references for tolerance allocation, i.e., sensitivity coefficient and percentage contribution.[44] They reflect the influences of individual tolerances on the FR in assemblies, and can be exchanged mathematically. Ghie et al.[34] explored a calculation method of percentage contribution in the unified Jacobian-Torsor model. However, it is not suitable for the modified method presented in this paper because it is in a deterministic way.

Generally, in a statistical context, the standard deviation of the FR is equal to the root sum square (RSS) of all FE's standard deviations. Therefore, the percentage contribution of the ith FE in the unified Jacobian-Torsor model in a statistical way can be expressed as:

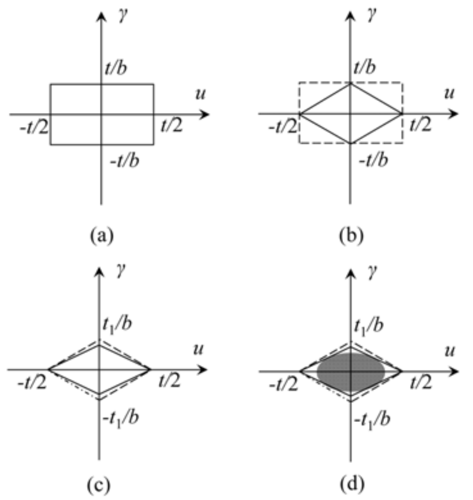

Fig. 10 Constraint relation between γ and $\boldsymbol{u}$ for a planar surface

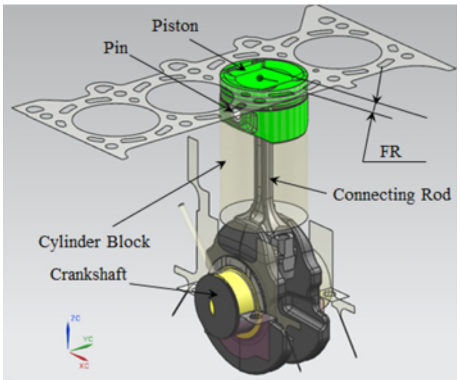

Fig. 11 FR of a crank-link mechanism of engine

$$PC_{FEi} = \frac{\sigma_{FEi}^2}{\sigma_{FR}^2} \tag{16}$$

where represents the standard deviation. σ_{FEi} is a statistical value of $[\boldsymbol{J_{FEi}} \times \boldsymbol{T_{FEi}}]$.

4. Case Study

In order to validate the modified method of the unified Jacobian-Torsor model, a crank-link mechanism of engine illustrated in Fig. 11 is studied. This mechanism which contains geometric tolerances and pin-hole joints is composed of five parts, i.e., cylinder block, crankshaft, connecting rod, piston and pin. Detailed drawings and reference frames of the first four parts are shown in Fig. 12. The pin is not illustrated because it is only specified with a diameter tolerance ($\phi 17^{0}_{-0.005}$). The FR (see Fig. 11) bounds the vertical displacement between two top planes of piston and cylinder block when the piston at its top dead center, which is an important parameter of the compression ratio of combustor in engines. The fluctuation of compression ratio has a strong impact on power, torque and fuel consumption of engines. The nominal value of FR in this example is 0.4 mm.

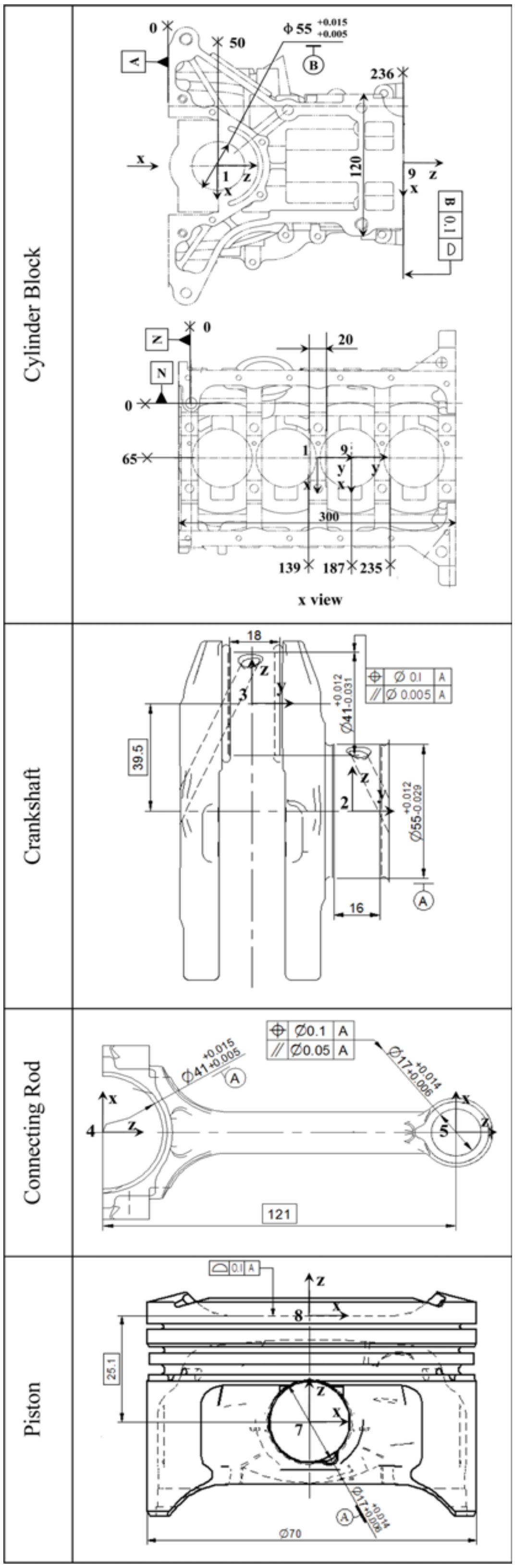

Fig. 12 Detailed drawing of parts

According to the principle of modified algorithm presented in the previous section, the computational process is as follows:

Step 1: Build the unified Jacobian-Torsor model. In this example, the reference frames are located in the middle of the tolerance or

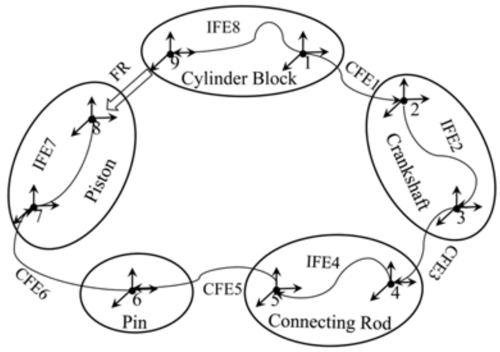

Fig. 13 Connection graph of crank-link mechanism

contact zones (see Fig. 12). Among them, reference 1 is the global reference frame where FR is calculated. The connection graph is shown in Fig. 13 where contact FE (CFE) and internal FE (IFE) are identified. Some CFEs are ignored in order to avoid parallel connections, such as the joint of piston and cylinder block.

Two unified Jacobian-Torsor models are established according to the connection graph. The first path is CFE1-IFE2-CFE3-IFE4-CFE5-CFE6-FE7, and the first Jacobian matrix is presented as Eq. (17). The second path contains only IFE8 and is not presented here.

$$
J_{FR1} = \left[\begin{bmatrix} 1&0&0&0&186&-48 \\ 0&1&0&-186&0&0 \\ 0&0&1&48&0&0 \\ 0&0&0&1&0&0 \\ 0&0&0&0&1&0 \\ 0&0&0&0&0&1 \end{bmatrix}_{FE1} \begin{bmatrix} 1&0&0&0&146.5&0 \\ 0&1&0&-146.5&0&0 \\ 0&0&1&0&0&0 \\ 0&0&0&1&0&0 \\ 0&0&0&0&1&0 \\ 0&0&0&0&0&1 \end{bmatrix}_{FE2} \begin{bmatrix} 1&0&0&0&146.5&0 \\ 0&1&0&-146.5&0&0 \\ 0&0&1&0&0&0 \\ 0&0&0&1&0&0 \\ 0&0&0&0&1&0 \\ 0&0&0&0&0&1 \end{bmatrix}_{FE3} \begin{bmatrix} 1&0&0&0&25.5&0 \\ 0&1&0&-25.5&0&0 \\ 0&0&1&0&0&0 \\ 0&0&0&1&0&0 \\ 0&0&0&0&1&0 \\ 0&0&0&0&0&1 \end{bmatrix}_{FE4} \begin{bmatrix} 1&0&0&0&25.5&0 \\ 0&1&0&-25.5&0&0 \\ 0&0&1&0&0&0 \\ 0&0&0&1&0&0 \\ 0&0&0&0&1&0 \\ 0&0&0&0&0&1 \end{bmatrix}_{FE5} \begin{bmatrix} 1&0&0&0&25.5&0 \\ 0&1&0&-25.5&0&0 \\ 0&0&1&0&0&0 \\ 0&0&0&1&0&0 \\ 0&0&0&0&1&0 \\ 0&0&0&0&0&1 \end{bmatrix}_{FE6} \begin{bmatrix} 1&0&0&0&0.4&0 \\ 0&1&0&-0.4&0&0 \\ 0&0&1&0&0&0 \\ 0&0&0&1&0&0 \\ 0&0&0&0&1&0 \\ 0&0&0&0&0&1 \end{bmatrix}_{FE7} \right] \tag{17}
$$

Step2: Establish variations and constraints of torsors. According to the subsection 3.1, eight torsors, along with their variations and constraints are established. This example contains three types of torsor models, i.e., IFEs of cylinder-plane and cylinder-cylinder, and CFEs of cylinder-cylinder. Table 1 lists three representative variations and constraints of torsor models.

Step 3: Generate random values for each component of torsor. The variations obtained in step 2 are used for the generation of random values for components of torsors. We assume that all components confirm to a normal distribution and all lengths confirm to a uniform distribution. The value of Z is 3, indicating that the reject rate is 0.27%. The randn() and rand() functions in Matlab® are used to generate the

Table 1 Variations and constraints of three torsor models

CFE1	Variations	$-0.044/2 \le u_1 \le 0.044/2$ $-0.044/2 \le w_1 \le 0.044/2$ $-0.044/96/2 \le \alpha_1 \le 0.044/96/2$ $-0.044/96/2 \le \gamma_1 \le 0.044/96/2$
	Constraints	$(w_1+\alpha_1 y)^2 + (u_1+\gamma_1 y)^2 \le 0.022^2$
IFE2	Variations	$-0.1/2 \le u_2 \le 0.1/2$ $-0.1/2 \le w_2 \le 0.1/2$ $-0.005/18/2 \le \alpha_2 \le 0.005/18/2$ $-0.005/18/2 \le \gamma_2 \le 0.005/18/2$
	Constraints	$(w_2+\alpha_2 y)^2 + (u_2+\gamma_2 y)^2 \le 0.05^2$
IFE8	Variations	$-0.1/2 \le w_8 \le 0.1/2$ $-0.1/300 \le \alpha_8 \le 0.1/300$ $-0.1/120 \le \beta_8 \le 0.1/120$
	Constraints	$-0.1/2 \le w_8+\beta_8 x+\alpha_8 y \le 0.1/2$ $-0.1 \le \beta_8 x+\alpha_8 y \le 0.1$

random values.

Step 4: Check the random value of each component of torsor with the constraint equations. This step make sure that all random values taken into computation accord with the tolerancing standard. The selection procedure described in Fig. 9 is realized by a program.

Step 5: Take the random values selected in step 4 into the modified model to computer the results of FR. In order to ensure the accuracy, the number of iterations is set as 10000 here.

Step 6: Analyze results of FR. We pay close attention to $\boldsymbol{w}$ of FR in this example. The mean and standard deviation of $\boldsymbol{w}$ are 2.1×10^{-4} and 0.0329 respectively, which are the sums of FR_1 and FR_2. With Eqs. (14)-(15), we obtain the tolerance of vertical displacement:

$$
\left.\begin{aligned} w_{SU} &= 2.1\times10^{-4}+3\times0.0329 = 0.09891 \\ w_{SL} &= 2.1\times10^{-4}-3\times0.0329 = -0.09849 \end{aligned}\right\} \tag{18}
$$

The results show that the vertical displacement between two top planes of piston and cylinder block lies in an interval of [0.30151, 0.49891].

It is worth mentioning that the computation of the modified method in a statistical way is almost instantaneous. Using an Intel Core (TM) 2, 1.83 GHz, 1.5 GB RAM computer, and performing 10000 iterations, time consumption of this model is 0.2 s.

The percentage contributions of eight FEs can be calculated according to Eq. (16). Only $\boldsymbol{w}$ of FR is needed to be calculated in this example. The derived contributions are normalized and listed in Fig. 14 in the order of their extents. APC in Fig. 14 denotes accumulative percentage contributions. This result is very useful to tolerance allocation or optimization of engines design.

5. Comparison and Discussion

An experiment has been carried out to verify the accuracy and reliability of the result presented in section 4. Five engines including twenty crank-link mechanisms in all have been picked out from assembly line randomly. Their structures and dimensions and tolerance specification were the same as the case in the previous section. The top dead center of each crank-link mechanism was determined by a rotational adjustment of crankshaft, which contained two steps. Step 1

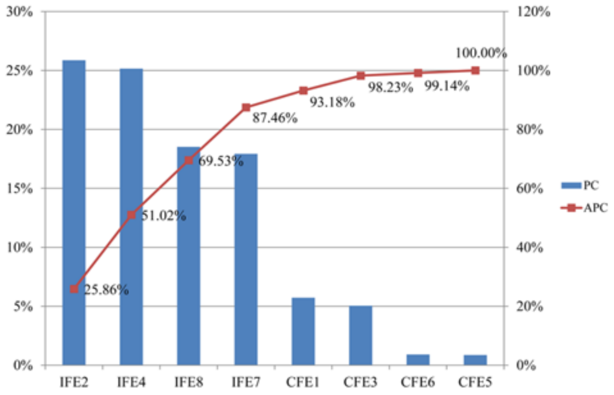

Fig. 14 Percentage contributions of eight FEs and their accumulative percentage contributions

Fig. 15 Adjustment and measurement of the experiment

found out its approximate location visually. Step 2 adjusted its accurate location by means of a dial gage, which needed a slight and slow rotational of crankshaft. These two steps shown in Fig. 15 were operated manually. After that, the actual distance between two top planes of piston and cylinder block was measured by a coordinate measuring machine (CMM). This CMM is provided by ZEISS®. Its accuracy limit is 1.4 m. It should be noted that the measure point of piston was assigned to the center of top plane of the piston, while the top plane of cylinder block was fitted by several points.

Because the top dead centers of four pistons were different, four cycles (location and measurement shown in Fig. 15) were needed to measure an engine. Measured data sets were [0.4997 0.4105 0.3978 0.4330 0.4208 0.4108 0.3631 0.3409 0.4019 0.4419 0.3800 0.4022 0.3823 0.4270 0.4028 0.3574 0.3753 0.3564 0.3880 0.3991], the unit of which was mm. Actual deviations of the FR were equal to the difference of measured data sets and the nominal distance (0.4 mm), the mean and standard deviation (Std) of which were listed in Table 2.

Table 2 lists five statistical results in the order of their ranges. Among them, the matrix model has been the mathematical basis of some widely used computer aided tolerancing software (CATs), such as CATIA.3D FDT®. The dimensional chain method is a traditional and mature method. The unified Jacobian-Torsor model is the original model introduced in section 2. We will make a detailed comparison from ranges and standard deviations of these results.

Table 2 Results of experiment and four methods

Order	Method	Result (mm)		
		Mean	Std	Range
1	Experiment	3×10^{-3}	0.0295	-0.0855, +0.0915
2	Modified unified Jacobian-Torsor model	2.1×10^{-4}	0.0329	-0.09849, +0.09891
3	Matrix model	1.8×10^{-4}	0.0333	-0.09972, +0.10008
4	Dimensional chain method	0	0.0353	-0.1058, +0.1058
5	Unified Jacobian-Torsor model	2.2×10^{-4}	0.0355	-0.10628, +0.10672

In order to make comparisons, the numerical order is used to represent the corresponding model or method. For example, Range (1) and Std (1) are the range and stand deviation of experiment respectively. Range (4) is set as the exact value because the dimensional chain method is a credible and well-developed method, and Range (1) obtained from the experiment is the actual value. As can be seen from Table 2, Range (2) obtained from the modified method of the unified Jacobian-Torsor model is narrower than Ranges (3-5) and wider than Range (1), which illustrates that the modified method we proposed is closer to the reality than other three models or methods. Range (5) is wide so much so that it is larger than Range (4), which confirms that taking limited values of both rotational and translational vectors into account is inaccurate. Furthermore, Std (5) is higher than Std (4) of about 0.6% and higher than Std (1) of more than 20.3%, while Std (2) is lower than Std (4) of 6.8% and higher than Std (1) of 11.5%. Std (5) is about 7.9% higher than Std (2). The comparative data explains that it is necessary to pay attention to the constraints between components of torsors in the unified Jacobian-torsor model.

Since the torsor model is the first order approximation of the matrix model,[40] Range (3) and Std (3) is nearly equal to Range (2) and Std (2) respectively. But they differ a lot in computational efficiency because the matrix model is constricted by a large number of inequalities. Based on the same computer, software, solution (Monte Carlo method) and the number of iterations, time consumption of the modified unified Jacobian-Torsor model is 0.2 s while that of the matrix model is 29 s.

The comparisons above show that the modified unified Jacobian-Torsor model presented in this paper is accurate, valid and effective.

The percentage contributions listed in Fig. 14 shows that IFE2, IFE4, IFE8 and IFE7 are the most important contributors in the crank-link mechanism of engines. It means that the tolerances of crankshaft, connecting rod, cylinder block and piston illustrated in Fig. 12 are very sensitive to the FR. The sum of four FEs' contributions is up to 87.46%. Tightening the first four FEs' tolerances and relaxing the last four FEs' tolerances may be a feasible way to arrive at a balance between the quality and the cost of engines manufacturing.

In addition, three statistical results of the assembly shown in Fig. 3 are listed in Fig. 16. They are obtained by the modified unified Jacobian-Torsor model, the dimensional chain method and the original Jacobian-Torsor model. Mean values are ignored because they are very small. As can be seen, Std (1) is lower than Std (2) of 4.7% while Std (3) is higher than Std (2) of 12.7%. Comparative results illustrate the accuracy and validity of the modified unified Jacobian-Torsor model again.

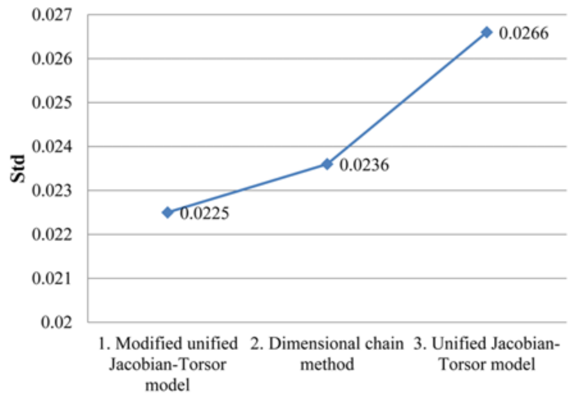

Fig. 16 Three statistical results of the assembly from Fig. 3

6. Conclusion

The attempt of the presented work was to propose a modified method for the unified Jacobian-Torsor model where the constraints between components of torsor were considered. The constraints are interactions of vectors caused by tolerances in a tolerance zone. Integrating them into consideration was very important to ensure the accuracy and reliability of the unified Jacobian-Torsor model. These inherent relations have been neglected before. The Monte Carlo method was used to solve this modified model in a statistical way. It was an efficient calculating method and was convenient for tolerance allocation. This method has been illustrated by a crank-link mechanism of engine and a two-block assembly. Comparative results showed that the modified method was accurate, valid and efficient.

Moreover, the constraints between translational vectors and rotational vectors, and the relation between dimensional tolerances and geometric tolerances presented in this paper, can be used for other 3D tolerance analysis models, such as the matrix model.

Although tolerance allocation in a statistical way has been introduced and illustrated, a great deal of work is needed to complete this modified method. The percentage contributions have just been quantified to each FE. The final objective is to distinguish clearly the percentage contribution of every tolerance of the FE, which will be detailed in further publications.

ACKNOWLEDGEMENT

The work described in this paper is supported in part by grants from the National Natural Science Foundation of China (Grant Nos. 51121063, 51175340) and the National Key Science and Technology Research Program of China (Grant No. 2014ZX04002011-3).

REFERENCES

1. Shen, Z., Ameta, G., Shah, J. J., and Davidson, J. K., “A Comparative Study of Tolerance Analysis Method,” Journal of Computing and Information Science in Engineering, Vol. 5, No. 3 pp. 247-256, 2005.
2. Hong, Y. S. and Chang, T. C., “A Comprehensive Review of Tolerancing Research,” International Journal of Production Research, Vol. 40, No. 11, pp. 2425-2459, 2002.
3. Chen, H., Jin, S., Li, Z., and Lai, X., “A Comprehensive Study of Three Dimensional Tolerance Analysis Methods,” Computer-Aided Design, Vol. 53, pp. 1-13, 2014.
4. Ameta, G., Serge, S. and Giordano, M., “Comparison of Spatial Math Models for Tolerance Analysis: Tolerance-Maps, Deviation, Domain, and TTRS,” Journal of Computing and Information Science in Engineering, Vol. 11, No. 2, Paper No. 012004, 2011.
5. Salomons, O. W., Haalboom, F. J., Poerink, H. J. J., Slooten, F. V., et al., “A Computer Aided Tolerancing Tool II: Tolerance Analysis,” Computers in Industry, Vol. 31, No. 2, pp. 175-186, 1996.
6. Portman, V. T., “Modelling Spatial Dimensional Chains for CAD/CAM Applications,” in: Computer-Aided Tolerancing, Kimura, F. (Ed.), Chapman & Hall, pp. 71-85, 1995.
7. Fleming, A., “Geometric Relationships between Toleranced Features,” Artificial Intelligence, Vol. 37, No. 1, pp. 403-412, 1988.
8. Rivest, L., Fortin, C., and Morel, C., “Tolerancing A Solid Model with A Kinematic Formulation,” Comput-Aided Design, Vol. 26, No. 6, pp. 465-476, 1994.
9. Lafond, P. and Laperrière, L., “Jacobian-based Modeling of Dispersions Affecting Predefined Functional Requirements of Mechanical Assemblies,” Proc. of IEEE International Symposium on Assembly and Task Planning, pp. 20-25,1999.
10. Davidson, J. K., Mujezinovic´, A., and Shah, J. J., “A New Mathematical Model for Geometric Tolerances as Applied to Round Faces,” Journal of Mechanical Design, Vol. 124, No. 4, pp. 609-622, 2002.
11. Gao, J., Chase, K. W., and Magleby, S. P., “General 3-D Tolerance Analysis of Mechanical Assemblies with Small Kinematic Adjustments,” IIE Transactions, Vol. 30, No. 4, pp. 367-377, 1998.
12. Bourdet, P., Mathieu, L., Lartigue, C., and Ballu, A., “The Concept of the Small Displacements Torsor in Metrology,” in: Series on Advances in Mathematics for Applied Sciences Advanced Mathematical Tools in Metrology, World Scientific Publishing, Vol. 40, pp. 110-122, 1996.
13. Clément, A., Desrochers, A., and Rivière, A., “Theory and Practice of 3D Tolerancing for Assembly,” Proc. of the CIRP Seminar on Computer Aided Tolerancing, pp. 25-55, 1991.
14. Desrochers, A. and Rivière, A., “A Matrix Approach to the Representation of Tolerance Zones and Clearances,” The International Journal of Advanced Manufacturing Technology, Vol. 13, No. 9, pp. 630-636, 1997.
15. Desrochers, A., Ghie, W., and Laperrière, L., “Application of a Unified Jacobian-Torsor Model for Tolerance Analysis,” Journal of Computing and Information Science in Engineering, Vol. 3, No. 1,

pp. 2-14, 2003.

16. Jin, J. and Shi, J., "State Space Modeling of Sheet Metal Assembly for Dimensional Control," Journal of Manufacturing Science and Engineering, Vol. 121, No. 4, pp. 756-762, 1999.
17. Anselmetti, B., "ISO Manufacturing Tolerancing: Three-Dimensional Transfer with Analysis Line Method," The International Journal of Advanced Manufacturing Technology, Vol. 61, No. 9-12, pp. 1085-1099, 2012.
18. Cai, W., Hu, S. J., and Yuan, J. X., "A Variational Method of Robust Fixture Configuration Design for 3D Workpieces," Journal of Manufacturing Science and Engineering, Vol. 119, No. 4A, pp. 593-602, 1997.
19. Mujezinovic´, A., Davidson, J. K., and Shah, J. J., "A New Mathematical Model for Geometric Tolerances as Applied to Polygonal Faces," Journal of Mechanical Design, Vol. 126, No. 3, pp. 504-518, 2004.
20. Davidson, J. K. and Shah, J. J., "Geometric Tolerances: A New Application for Line Geometry and Screws," Proceedings of the Institution of Mechanical Engineers, Part C: Journal of Mechanical Engineering Science, Vol. 216, No. 1, pp. 95-103, 2002.
21. Bhide, S., Davidson, J. K., and Shah, J. J., "A New Mathematical Model for Geometric Tolerances as Applied to Axes," Proc. of ASME 2003 International Design Engineering Technical Conferences and Computers and Information in Engineering Conference, pp. 329-337, 2003.
22. Bhide, S., Ameta, G., Davidson, J. K., and Shah, J. J., "Tolerance-Maps Applied to the Straightness and Orientation of an Axis," in: Models for Computer Aided Tolerancing in Design and Manufacturing, Davidson, J. K. (Ed.), Springer, pp. 45-54, 2007.
23. Ameta, G., Davidson, J. K., and Shah, J. J., "The Effects of Different Specifications on the Tolerance-Maps for an Angled Face," Proc. of ASME International Design Engineering Technical Conferences and Computers and Information in Engineering Conference, pp. 303-311, 2004.
24. Ameta, G., Davidson, J. K., and Shah, J. J., "Tolerance-Maps Applied to a Point-line Cluster of Features," Journal of Mechanical Design, Vol. 129, No. 8, pp. 782-792, 2007.
25. Ameta, G., Davidson, J. K., and Shah, J. J., "Using Tolerance-maps to Generate Frequency Distributions of Clearance and Allocate Tolerances for Pin-hole Assemblies," Journal of Computing and Information Science in Engineering, Vol. 7, No. 4, pp. 347-359, 2007.
26. Ameta, G., Davidson, J. K., and Shah, J. J., "Influence of Form on Tolerance-Map-generated Frequency Distributions for 1D Clearance in Design," Precision Engineering, Vol. 34, No. 1, pp. 22-27, 2010.
27. Ameta, G., Davidson, J. K., and Shah, J. J., "Effects of Size, Orientation, and Form Tolerance on The Frequency Distributions of Clearance between Two Planar Faces," Journal of Computing and Information Science in Engineering, Vol. 11, No. 1, Paper No. 011002, 2011.
28. Whitney, D. E., Gilbert, O. L., and Jastrzebski, M., "Representation of Geometric Variations using Matrix Transforms for Statistical Tolerance Analysis in Assemblies," Research in Engineering Design, Vol. 6, No. 4, pp.191-210, 1994.
29. Chase, K. W., Gao, J., and Magleby, S. P., "General 2-D Tolerance Analysis of Mechanical Assemblies with Small Kinematic Adjustments," Journal of Design and Manufacturing, Vol. 5, No. 4, pp. 263-274, 1995.
30. Chase, K. W., Gao, J., Magleby, S. P., and Sorensen, C. D., "Including Geometric Feature Variations in Tolerance Analysis of Mechanical Assembly," IIE Transactions, Vol. 28, No. 10, pp. 795-807, 1996.
31. Glancy, C. G. and Chase, K. W., "A Second Order Method for Assembly Tolerance Analysis," Proc. of ASME Design Engineering Technical Conferences, Paper No. DETC99/DAC-8707, 1999.
32. Laperrière, L., Ghie, W., and Desrochers, A., "Statistical and Deterministic Tolerance Analysis and Synthesis using a Unified Jacobian-Torsor Model," CIRP Annals - Manufacturing Technology, Vol. 51, No. 1, pp. 417-420, 2002.
33. Ghie, W., Laperrière, L., and Desrochers, A., "Statistical Tolerance Analysis using the Unified Jacobian-Torsor Model," International Journal of Production Research, Vol. 48, No. 15, pp. 4609-4630, 2010.
34. Ghie, W., Laperrière, L. and Desrochers, A., "Re-design of Mechanical Assembly using the Unified Jacobian-Torsor Model for Tolerance Analysis," in: Models for Computer Aided Tolerancing in Design and Manufacturing, Davidson, J. K. (Ed.), Springer, pp. 95-104, 2007.
35. The American Society of Mechanical Engineers, "Dimensioning and Tolerancing," ASME Y14.5, 2009.
36. Teissandier, D., Couétard, Y. and Gérard, A., "A Computer Aided Tolerancing Model: Proportioned Assembly Clearance Volume," Computer-Aided Design, Vol. 31, No. 3, pp. 805-817, 1999.
37. Salomons, O. W., "Computer Support in The Design of Mechanical Products," Ph.D. Thesis, Department of Mechanical Engineering, University of Twente, pp. 211-242, 1995.
38. Laperrière, L. and Desrochers, A., "Modeling Assembly Quality Requirements using Jacobian or Screw Transforms: A Comparison." Proc. of the IEEE International Symposium on Assembly and Task Planning, pp. 330-336, 2001.
39. Marziale, M. and Polini, W., "A Review of Two Models for Tolerance Analysis of an Assembly: Jacobian and Torsor," International Journal of Computer Integrated Manufacturing, Vol. 24, No. 1, pp. 74-86, 2011.
40. Desrochers, A., "Modeling Three Dimensional Tolerance Zones using Screw Parameters," Proc. of ASME Design Automation Conference, pp. 895-903, 1999.

41. Cai, M., Yang, J. X., and Wu, Z. T., "Mathematical Model of Form Tolerance for Cylindrical Feature based on Mathematical Definition," Chinese Journal of Mechanical Engineering, Vol. 39, No. 12, pp. 86-90, 2003.

42. Roy, U. and Li, B., "Representation and Interpretation of Geometric Tolerances for Polyhedral Objects. II. Size, Orientation and Position Tolerances," Computer-Aided Design, Vol. 31, No. 4, pp. 273-285, 1999.

43. Nigam, S. D. and Turner, J. U., "Review of Statistical Approaches to Tolerance Analysis," Computer-Aided Design, Vol. 27, No. 1, pp. 6-15, 1995.

44. Lin, C. H., Huang, W. H., Jeng, M. C., and Doong, J. L., "Study of an Assembly Tolerance Allocation Model based on Monte Carlo Simulation," Journal of Materials Processing Technology, Vol. 70, No. 1, pp. 9-16, 1997.